

# A Toroidal Magnetic Spacecraft Shield

Simon G. Shepherd\*

*Thayer School of Engineering, Dartmouth College, Hanover, New Hampshire, 03755*

John P. G. Shepherd<sup>†</sup>

*Department of Physics, University of Wisconsin, River Falls, Wisconsin, 54022*

The use of magnetic fields to deflect energetic charged particles has been proposed as a means to protect astronauts from the harmful radiation encountered in space. These so-called active magnetic shields must provide a region of space which is protected from energetic particles below a given energy while also maintaining a safe level of magnetic field strength within the shielded region. A toroidally shaped environment with circular coils of wire distributed on the surface of the spacecraft is shown to satisfy these requirements. Numerical techniques are used to demonstrate that particles below a given energy, including galactic cosmic rays (GCRs), are completely shielded from a region inside the toroidal spacecraft. By choosing the appropriate amplitudes of the currents flowing in the circular coils, the magnetic field-strength inside this region can also be made arbitrarily small inside the toroidal spacecraft. While many practical issues must be addressed with this design, it has been demonstrated that it is indeed possible to construct a magnetic field suitable for protecting astronauts from GCRs during long-duration manned missions.

## Nomenclature

$\vec{A}$	vector potential of the magnetic field
$A_\phi$	$\phi$ component of the vector potential
$\alpha$	angle around spacecraft cross-section
$a$	radius of coil
$B$	magnetic flux density
$\vec{B}_{\text{in}}$	vector magnetic flux density inside boundary
$\vec{B}_{\text{out}}$	vector magnetic flux density outside boundary
$C_{st}$	Störmer length
$c$	speed of light
$\gamma$	Lorentz relativistic correction factor
$I$	electrical current in coil
$\vec{J}$	surface current density
$\lambda$	magnetic latitude
$\mathcal{L}$	relativistic Lagrangian of a particle
$L$	inductance
$\mu_0$	permeability of free space
$M$	magnitude of magnetic dipole moment
$\vec{M}$	vector magnetic dipole moment
$m_0$	rest mass of particle
$n$	number of turns of wire
$\hat{n}$	unit vector normal to boundary
$\hat{\phi}$	$\phi$ unit vector

---

\*Research Associate Professor, Thayer School of Engineering, Dartmouth College, 8000 Cummings Hall, Hanover, New Hampshire 03755-8000, Member AIAA.

<sup>†</sup>Professor Emeritus, Department of Physics, University of Wisconsin, River Falls, Wisconsin 54022

$p_\phi$	$\phi$ component of the generalized momentum
$q$	electrical charge of the particle
$\vec{v}$	vector velocity of particle
$v$	speed of particle
$\rho$	radius in standard cylindrical coordinates
$R$	magnetic rigidity of a particle
$r, \theta, \phi$	radius and angles in standard polar coordinates
$\dot{r}, \dot{\theta}, \dot{\phi}$	generalized velocities associated with the $r, \theta, \phi$ coordinates
$r_b$	radius of circular approximation to cross-section of torus
$r_c$	radius to center of circular cross-section approximation
$s$	distance along magnetic field-line
$x, y, z$	standard rectangular coordinates

## I. Introduction

The need to protect astronauts from the harmful effects of space radiation in the form of energetic particles is a problem that must be addressed if manned missions of extended duration, such as those to Mars, are to become reality. The most harmful of these particles are solar energetic particles (SEPs) resulting from large solar flares and galactic cosmic rays (GCRs) originating from outside our solar system. While the particle flux of each population falls off steeply with increasing energy, SEPs are typically <100 MeV per nucleon and the GCR spectrum peaks around 1 GeV per nucleon before falling off.<sup>1-3</sup> While there is considerable uncertainty in assessing the risks to astronauts from these energetic particles, it is generally agreed that particles with energies of 1-4 GeV per nucleon are the most damaging to humans.<sup>4-7</sup>

Traditional techniques for protecting spacecraft from these forms of radiation typically involve a protective shield of material used to absorb the energy of incoming particles. While these so-called passive shields can be effective at blocking particles with lower energies, the mass required for protecting against energetic particles such as GCRs becomes impractical for use in spacecraft. In addition, higher energy particles colliding with a passive shield produce a cascade of lower energy particles that could be even more damaging to human cells than the original particles. For these reasons an active shield which utilizes electric or magnetic fields to deflect energetic particles is a possible alternative for long-duration, manned missions. A review of active shields was performed by Sussingham et al.<sup>8</sup>

Several concepts for these so-called active shields have been proposed including electrostatic shields<sup>9,10</sup> and magnetic shields, that either include an artificial plasma environment<sup>11</sup> or that do not.<sup>6,12-14</sup> Electrostatic shields are generally considered to be impractical for shielding GCR particles due to the difficulties of generating a sufficiently high-voltage potential and are too dangerous in situations of accidental discharge.<sup>13</sup>

Magnetic shields can be roughly divided into those which rely solely on magnetic fields to deflect particles and those which have an artificial plasma environment that acts to inflate the existing magnetic field. The primary advantage of an artificial plasma environment is the claim that particles of a given energy are deflected using a much lower magnetic field-strength than would be required using a magnetic field only.<sup>11</sup> There is, however, some question as to the effectiveness of such a device to shield particles, particularly along the magnetic field axis.<sup>15</sup> Whether such a concept works as an effective shield or not, the addition of an artificial plasma clearly represents an increase in complexity of the overall design that we avoid in further discussion.

Shields which rely strictly on static magnetic fields to deflect charged particles via the Lorentz force can be further categorized as either confined or deployed, depending on the configuration of the current carrying wires (or coils) relative to the habitable portion of the spacecraft. Deployed magnetic shields rely on a configuration of coils (the simplest being a circular coil of radius  $a$ ) that are located at large distances from the spacecraft. The main advantage of a deployed shield is that the amount of electrical current ( $I$ ) needed to sustain a given magnetic dipole moment magnitude ( $M = I\pi a^2$ ) decreases as the size of the coil increases.<sup>12, 16-18</sup> It has been shown, however, that the shielding capacity of such coils is also reduced significantly to the extent that no shielding of the type that is expected actually occurs in a region near the center of the coil.<sup>19, 20</sup>

Confined magnetic shields, on the other hand, are so named for the coils being located in close proximity to, or even as an integral part of, the spacecraft living area.<sup>6, 14, 21-23</sup> In these devices it has been shown

that by using sufficiently large electrical currents it is possible to shield the entire spacecraft from energetic particles. For some of these devices, however, the magnetic field-strength produced by the coils that is necessary to protect from GCR particles is extraordinarily high ( $>10$  T) in the vicinity that is being shielded. While it is relatively unknown what the effects of high-strength static magnetic fields are on humans, there are many reports of individuals experiencing various neurological effects while in motion near magnetic resonance imaging (MRI) machines with magnetic field-strengths  $<10$  T.<sup>24,25</sup>

A dilemma of sorts seems to exist with the design of confined magnetic spacecraft shields in that a high magnetic field-strength is needed to deflect energetic GCR particles yet a low field-strength is desired for the safety of the spacecraft occupants. One solution to this problem is to confine the magnetic field to a relatively small region around the spacecraft.<sup>6,14</sup> We propose an alternate solution which satisfies both of these apparently contradictory design requirements. The device we propose consists of a toroidally-shaped spacecraft, with a non-circular cross-section in the  $\rho$ - $z$  plane, where  $\rho^2 = x^2 + y^2$  defines the polar coordinate (see Fig. 1). Circular wires (coils) are located around the exterior of the spacecraft through which electrical current flows in the toroidal direction, providing the magnetic field necessary to deflect energetic particles. By adjusting the strength of the currents flowing in each coil it is possible to create a magnetic field that is both large exterior to the spacecraft (thereby shielding the occupants) and arbitrarily small inside the spacecraft (thereby providing a non-hazardous environment).

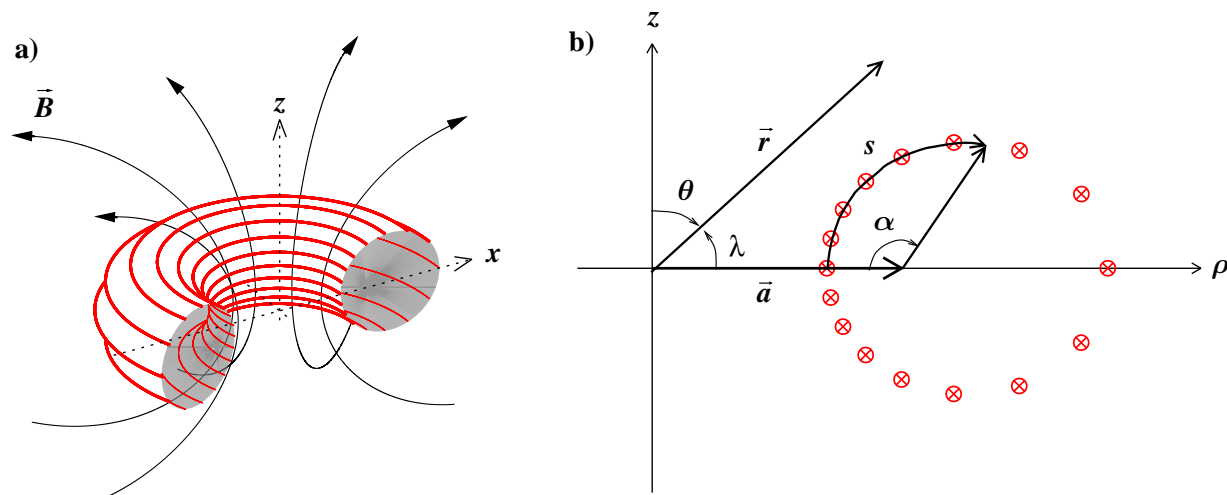


Figure 1. (a) Cut-away view of a toroidally-shaped spacecraft with 16 conducting wire loops, shown as solid thick lines, located on the surface of the spacecraft. Representative magnetic field lines are indicated by solid lines with arrows. (b) A view of the spacecraft cross-section in the  $\rho$ - $z$  plane showing the coordinate system and locations of the wires uniformly spaced in the angle  $\alpha$ . The vector  $\vec{a}$ , described in the text and shown as a cross symbol in Fig. 2 and Fig. 3, is the radius of a single coil which defines the external magnetic field.

The remainder of the paper is organized as follows, section II examines the shielded region produced by a single coil of wire which motivates the use of toroidally-shaped spacecraft. The shielded regions are determined using two numerical techniques, the first involving numerical solutions of the generalized azimuthal angular momentum of a particle moving in a magnetic field, and the second a test-particle simulation in which particle trajectories are calculated. Section III introduces the shape of the toroidal spacecraft and the configuration of coils that allows the magnetic field to be reduced to zero inside the spacecraft. A discussion of the shielding capabilities of the toroidal spacecraft is presented in section IV in addition to some of the many practical considerations for building such a spacecraft. Finally, a summary is given in section V.

## II. Shielded Region Due to Circular Coil

The motivation for the design of toroidally-shaped spacecraft comes in part from the analysis of particle trajectories in the presence of magnetic fields. For certain configurations the influence these magnetic fields impart on charged particles through the Lorentz force can lead to regions of space for which particles below a given energy do not have access, or are forbidden. These regions of space are said to be shielded from such

particles.

Derivations of these regions, similar to the one described here, have been presented before.<sup>26–28</sup> We begin a brief derivation with the relativistic Lagrangian of a particle of mass  $m_0$  and charge  $q$ , moving with velocity  $\vec{v}$  in a static magnetic field with vector potential  $\vec{A}$  and in the absence of an electric field.<sup>29</sup> If the magnetic field is axially symmetric about the  $z$  axis, i.e.,  $\vec{A} = A_\phi \hat{\phi}$  in polar coordinates, then

$$\mathcal{L} = -\gamma^{-1}m_0c^2 + qA_\phi r \sin \theta \dot{\phi} \quad (1)$$

where  $\gamma = (1 - v^2/c^2)^{-1/2}$  is the Lorentz relativistic correction factor,  $c$  is the speed of light,  $r$  is the radial distance from the origin to the particle in spherical coordinates,  $\theta$  is the angle from the  $z$  axis,  $\dot{\phi}$  is the generalized velocity associated with the  $\phi$  coordinate, and SI units are used throughout.

Because equation (1) is independent of  $\phi$ , the Lagrangian equation of motion for the  $\phi$  coordinate can be written as

$$\frac{d}{dt}p_\phi = \frac{\partial \mathcal{L}}{\partial \phi} = 0 \quad (2)$$

and  $p_\phi$  is, therefore, a constant of the motion given by

$$p_\phi = \frac{\partial \mathcal{L}}{\partial \dot{\phi}} = -m_0c^2 \frac{\partial \gamma^{-1}}{\partial v} \frac{\partial v}{\partial \dot{\phi}} + qA_\phi r \sin \theta \quad (3)$$

Using  $v^2 = \dot{r}^2 + r^2\dot{\theta}^2 + r^2 \sin^2 \theta \dot{\phi}^2$  to evaluate the partial derivatives in equation (3), the azimuthal component of the generalized momentum can be written as

$$p_\phi = \gamma m_0 v_\phi r \sin \theta + qA_\phi r \sin \theta \quad (4)$$

A closed-form solution to equation (4) has been shown to exist for only a few special magnetic field configurations. Carl Störmer showed that such a solution existed for a pure dipole magnetic field.<sup>30</sup> Inserting the vector potential of a pure dipole  $A_\phi = -(\mu_0/4\pi)M \sin \theta/r^2$ , with dipole moment  $\vec{M} = M\hat{z}$  into equation (4), the equation describing the shielded region of a magnetic dipole located at the origin is given by

$$r = \sqrt{\frac{Mq\mu_0}{4\pi\gamma m_0 v} \frac{\cos^2 \lambda}{1 + \sqrt{1 + \cos^3 \lambda}}} \quad (5)$$

where  $\lambda$  is the magnetic latitude ( $\pi/2 - \theta$ , see Fig. 1). The factor in front of the radical in equation (5) has units of length and is often referred to as the Störmer length, given by

$$C_{st} \equiv \sqrt{\frac{Mq\mu_0}{4\pi\gamma m_0 v}} = \sqrt{\frac{M}{R} \frac{\mu_0}{4\pi}} \quad (6)$$

which can be written in terms of the magnitude of the dipole moment  $M$  and the so-called rigidity of the particle,  $R \equiv \gamma m_0 v/q$ .

Equation (5) describes a toroidal shielded region around the origin. In the equatorial plane ( $\lambda = 0^\circ$ ) the region extends a distance approximately  $0.4C_{st}$ . Along the axis of the dipole ( $\lambda = \pi/2$ ) however, the distance of this region is zero, i.e., no shielding occurs for particles moving along the axis of the dipole. Regardless of the magnitude of the dipole moment  $M$ , it is therefore not possible to completely shield a region of any size at the origin from particles of any energy. For this reason it is more sensible to build a spacecraft that is more congruent with the geometry of the shielded region, i.e., toroidal. In this case, shielding particles that are traveling along trajectories near the axis of the dipole is not an issue as they pass harmlessly through the center of the toroidal spacecraft.

Several confined magnetic shields of this design have been proposed.<sup>22, 23, 31</sup> In these cases, however, the dipole magnetic field is approximated by the field due to a coil of finite radius  $a$  with  $n$  turns of wire each carrying a current of  $I$ . The magnetic field of such a coil provides shielding of the type described in equation (5) only when  $a \ll C_{st}$ .<sup>19, 20</sup>

Shielding also occurs for situations in which  $a \geq C_{st}$ , however not of the type described by equation (5), i.e., the dipole approximation is not valid. In order to determine the shielded region due to a coil of wire,

equation (4) must be solved using the vector potential  $A_\phi$  of the coil. Levy<sup>27</sup> shows that while it is not possible to write a closed-form solution to this equation, a numerical solution is possible.

Figure 2 shows the shielded regions calculated using this numerical technique for three different idealized coils of radii:  $a = 3.415$  m,  $9.115$  m,  $14.35$  m. The location of the single coil is shown by the circular symbol with a cross, indicating that the current flows into the page, and the wire is assumed to have no thickness. Protons with energy 1 GeV or less are forbidden from the toroidal region around the coils that are described by the curves shown. The total current required to shield such particles in each case is  $nI = 6.451 \times 10^8$  A,  $1.688 \times 10^8$  A, and  $1.071 \times 10^8$  A for Fig. 2a, 2b, and 2c, respectively. For reference, the strength of the magnetic field in each case is indicated by the logarithmic greyscale contours.

Also shown in Fig. 2 are the positions of representative 1 GeV  $H^+$  (protons) test particles at their closest approach to the coil. Particle trajectories are calculated using a numerical technique described by Shepherd and Kress.<sup>19</sup> Briefly, the coupled set of differential equations describing the motion of a particle of given energy, mass, and charge in the presence of an external magnetic field are solved using a standard Runge-Kutta 4<sup>th</sup>-order method. To accurately resolve the particle trajectories an adaptive time-step is used by adjusting the step size to be 0.1% of the instantaneous gyroperiod of the particle. A maximum step size of  $1 \mu s$  is used, but no lower bound on the minimum step size is imposed. While this numerical technique does not explicitly conserve adiabatic invariants it has been demonstrated to accurately resolve shielded regions and geomagnetic cutoffs due to static magnetic fields.<sup>19, 20, 32, 33</sup>

As shown in Fig. 2, agreement between the boundaries determined using two entirely different numerical techniques is excellent. While many test-particles come within a small fraction of 1 m to the boundary, no particle penetrates this region. For these simulations, particles are initiated at random positions uniformly distributed on a sphere of radius 1 km. In order to sample the possible trajectories that could penetrate the region near the coil, particles are initiated with velocities according to their energy (1 GeV) and directed toward another random point on a sphere of radius 500 m centered at the origin. The resulting sampling of test-particle trajectories is not intended to represent a true distribution function, but rather an appropriate sample that reveals any shielded regions located near the coils.

Figure 2 shows that a spacecraft enclosing the coil would contain a shielded region near the coil to which particles of a given energy do not have access. Toroidal spacecraft of this design have been proposed.<sup>23</sup> The main problem with these designs is that the strength of the magnetic field required to deflect GCR particles is very large. This field is strongest near the coil, which is enclosed within the spacecraft thereby exposing the occupants to very large static magnetic fields. The field strength inside the shielded regions shown in Fig. 2 is  $>3$  T and a minimum on the shielded surface itself. Moving away from the boundary toward the location of the coil, the field becomes unbounded.

Documented studies show exposure to static magnetic fields as low as  $\sim 0.1$  T can affect blood flow around the heart, however the physiological consequences of this interaction are unclear.<sup>34</sup> While it is likely that long-term exposure to static magnetic fields would pose a serious health risk to astronauts, no studies of long-term exposure exist. The best available data on health risks associated with exposure to static magnetic fields come from laboratory and epidemiological studies involving magnetic resonance imaging (MRI) and spectroscopy (MRS) technicians. While no threshold has been set for continuous exposure to static magnetic fields, the National Radiological Protection Board (NRPB), and other international agencies, have set occupational guidelines for working with MRI in the form of time-weighted-average field exposure of 0.20 T per 8-hour workday.<sup>24</sup> Although the effects of constant exposure to such fields over long durations is unknown, extrapolation of the NRPB recommendations would suggest that the magnetic field strength inside the spacecraft should not exceed a level of  $\sim 70$  mT.

### III. Magnetic Field Cancellation

For the example of a toroidally-shaped spacecraft, that is suggested by the shielded regions shown in Fig. 2, it is therefore desired to reduce the field inside the torus (the shielded region) while leaving the field external to the spacecraft unchanged. Reduction of the magnetic field can be accomplished by adding additional coils in such a configuration that the magnetic fields oppose the field of the main coil, thereby canceling the field in the desired region. A relatively simple solution is to add a single coil that is coplanar to the main coil but with a smaller radius. The strength of the current in the secondary coil is chosen so that the superposition of the fields is zero on a circular path between the two coils.<sup>35</sup>

While this particular configuration is relatively simple and reduces the field in the region between the

two coils, it also affects the fields out of the plane of the coils. Particles penetrating the region of space near the coils can have very complicated three-dimensional trajectories. Shielding of these particles is achieved by the detailed magnetic field near the coils, rather than by the overall magnetic moment.<sup>19</sup> Reducing the field in this manner can, therefore, also have the effect of reducing the shielding capacity for some particle trajectories. It is possible, in principle, to reduce the field inside the torus to exactly zero, everywhere, without affecting the field external to the spacecraft.

In order to show how such a configuration of coils is possible, we first determine the cross-sectional shape of the torus by computing a magnetic field-line of the single coil shown in Fig. 2b. Figure 3 is a reproduction of Fig. 2b with the addition of four magnetic field-lines computed from starting positions of  $z = 0$  m and  $\rho = 2$  m, 4m, 6 m, and 7.342 m. The latter field-line (indicated by a thicker line) is chosen to represent a region that extends 5.0 m in the vertical ( $z$ ) direction and is centered at  $\rho = 10.0$  m. These dimensions represent a possible spacecraft design that would provide adequate space inside the torus for habitation.

The cross-sectional shape of the spacecraft is chosen to correspond to the shape of the magnetic field-line represented by the thicker line. In this configuration, the magnetic field, by definition, is tangential everywhere to the surface of the spacecraft. The magnetic field inside the spacecraft can be made to be exactly zero everywhere by specifying an appropriate surface current density  $\vec{J}$  that flows along the outer surface of the spacecraft in the toroidal direction ( $\hat{\phi}$ ). The surface current density  $\vec{J}$  is determined by invoking Ampere's Law at the boundary of the spacecraft. In this case the jump in the tangential magnetic field at a boundary is proportional to the surface current density flowing along the boundary,<sup>36</sup> or

$$\hat{n} \times (\vec{B}_{\text{out}} - \vec{B}_{\text{in}}) = \mu_0 \vec{J} \quad (7)$$

where  $\hat{n}$  is the normal to the magnetic field or spacecraft surface,  $\vec{B}_{\text{in}}$  and  $\vec{B}_{\text{out}}$  are the magnetic field vectors on the inner and outer edge of the spacecraft surface, and  $\vec{J}$  is the surface current density in A m<sup>-1</sup> flowing in the  $\hat{\phi}$  direction along the surface of the spacecraft.

By choosing the magnetic field to be zero on the inner edge of the boundary,  $\vec{B}_{\text{in}} = 0$ , equation (7) can be solved for the surface current density that is needed to produce the desired magnetic field,

$$\vec{J} = \frac{B_{\text{out}}}{\mu_0} \hat{\phi} \quad (8)$$

Using the magnetic field resulting from the single coil along the spacecraft surface for  $B_{\text{out}}$ , equation (8) gives the surface current density which produces the same magnetic field outside the spacecraft as the single coil, but the field inside the spacecraft is everywhere zero. Such a magnetic field provides shielding against particles below a certain energy without the associated high field strengths within the spacecraft that are associated with many confined magnetic shields.

The solid line in Fig. 4 shows the current density  $J$  as a function of distance along the field-line that is needed to produce the desired fields for the configuration shown in Fig. 3. As shown in Fig. 1 and Fig. 3, the distance along the field-line is given by  $s$ , measured from the location on the spacecraft surface closest to the origin. The total current,  $J$  integrated around the entire field-line, is within 0.1% of the value determined for the single coil;  $1.688 \times 10^8$  A.

The practical issue of controlling the distribution of current that flows along the surface of the spacecraft can be achieved by approximating the current density  $J$  with discrete wires or coils located around the surface of the spacecraft. The current flowing in each coil is determined by integrating the current density along the line segment (in the  $s$  direction) that extends half the distance to the adjacent coils. The dots in Fig. 4 indicate the positions of 32 circular coils distributed around the surface of the spacecraft and the current required in each coil. The 32 coils are distributed uniformly in the angle  $\alpha$  around the surface (See Fig. 1). The total current in the 32 coils is again within 0.1% of the current in the single coil shown in Fig. 3.

As expected, the discrete approximation to the current density  $J$  leads to imperfect cancellation of the magnetic field inside the torus and the approximation improves by using more coils. Fig. 5 shows the magnetic field in the vicinity of the spacecraft that results from 8, 16, 32, and 64-coil approximations. The magnitude of the magnetic field is represented in Fig. 5 by the logarithmic greyscale. Locations of the coils are indicated by the circular symbol containing a cross, indicating the current flowing into the page. The magnitude of the current in each coil varies according to the curves in Fig. 4.

As shown in Fig. 5 the field is not exactly zero everywhere inside the torus for the various approximations shown. The field, however, is significantly reduced from that of the single coil shown in Fig. 2b. The reduction

obtained with the 8-coil approximation is the least accurate of the four cases shown in Fig. 5, however, even for this relatively poor approximation the field is less than 2 T everywhere within a small fraction of a meter inside the spacecraft. Recall that in the case of the single coil the field was greater than 3 T at the boundary and increased without limit for locations approaching the coil. The cancellation improves with each doubling of the number of coils. Near complete cancellation is achieved for the 64-coil approximation shown in Fig. 5d. The field-strength in this case is less than 0.01 T at all locations inside the torus that are at least a distance of  $\sim 0.3$  m from the interior surface of the spacecraft. As the number of coils approaches infinity the cancellation becomes exact and the field everywhere inside the toroidal volume comprising the spacecraft decreases to zero.

## IV. Discussion

The discrete nature of the approximation to equation (8) is evident in the magnetic field produced by the multiple coil design (torus), particularly with the 8-coil example shown in Fig. 5a. In this example the differences between the magnetic fields of the torus and the single coil are most apparent. At large distances from the surface of the spacecraft the field from the multiple coils approximates the field from the single coils to very good agreement. In a region surrounding the coils that extends a distance roughly equal to the separation between the coils, the agreement breaks down.

The implication is that for a shielded region, which extends beyond the surface of the spacecraft by a distance that is larger than the separation between the coils, the field that any particle will experience along its trajectory will be equivalent to that of the single coil. For such cases the shielded region for the multiple coil design can be obtained by solving equation (4) using the much simpler form of the vector potential  $A_\phi$  for the single coil. Several studies use this approximation to describe the regions shielded by multiple coil designs.<sup>27, 37</sup>

For situations in which particle trajectories approach the surface of the spacecraft within a distance that is approximately equal to the separation between coils, the particle will experience a different magnetic field from the single coil, and differences in the shielded regions will, therefore, exist. It is possible in such situations to solve equation (4) using the full vector potential  $A_\phi$  for the multiple coils. Figure 6 shows the shielded regions calculated using the multiple coil vector potential for the 8-coil and 32-coil examples shown in Figs. 5a and 5c. As with the other examples, the corresponding test-particle simulations show excellent agreement with the numerically determined shielded regions.

For these examples the total current was chosen such that the shielded region for a 1 GeV proton would be 1 m from the outermost point of the single coil configuration. Due to the proximity of the shielded region to the surface of the spacecraft, small differences are visible between the single and multiple coil regions shown in Figs. 2c and 5. To better quantify the single coil approximation, Figure 7 shows the radial difference between the boundary determined using multiple coils and the single coil as a function of the angle  $\alpha$ . In general, Fig. 7 shows the shielded region of multiple coils approaches that of the single coil in a roughly linear fashion as the number of coils increases.

Shielded regions of larger or smaller dimensions may be determined by increasing or reducing the current in each coil proportionately. It is possible to reduce the current in the single coil to the extent that a portion or all of the shielded region is contained inside the surface of the desired spacecraft. In such cases particles have access to the interior of the spacecraft where the magnetic field is very low. The shielded region of the single wire is no longer a valid approximation in these situations. Shielded regions do exist under these conditions, however, the geometry of the region or regions due the multiple coils can be rather complex.

While it has been demonstrated that a magnetic field configuration can be constructed such that a region of very low magnetic field is contained entirely within a region for which particles below a given energy are forbidden access, there remain numerous practical issues for implementing such a design. Foremost is the large current required to shield GCR particles. For the examples shown in Fig. 2 the current required to shield 1 GeV protons from the toroidal spacecraft are  $>10^8$  A. It is expected that superconducting coils would be required to minimize the significant electrical resistance and dissipation that is expected for such large currents. The magnitude of the required current can be somewhat reduced by using multiple turns of wire in each coil and increasing the number of coils used to generate the magnetic field. Even with these measures, however, it is unlikely that such large currents can be achieved with modern superconducting technology. Significant advancements in this area will be needed before this limitation can be overcome.

Using multiple coils and multiple turns of wire has the advantage of reducing the current required in each

wire, however, it also adds weight to the spacecraft. Superconducting coils would also require additional cooling apparatus and perhaps structural reinforcement, all which adds further to the weight of the spacecraft. Although it is difficult to estimate how much additional weight is necessary for such a design, Levy<sup>21</sup> showed that the weight-reducing benefit of magnetic shields relative to passive shields was most significant for GCR particles. An analysis of the weight requirements depends on the details of how the coils are designed, but is necessary to ensure that weight reduction is significant enough to warrant the added complexity of a magnetic shield.

Another practical concern about the feasibility of such a device is the amount of energy required to power the shield. The energy stored in the magnetic field of an inductor is given by  $E = LI^2/2$ , where  $L$  is the inductance of the device and  $I$  is the total current flowing through the inductor. While an accurate determination of this energy requires detailed calculations of magnetic flux surfaces for the toroidal coils, an approximate value can be obtained by assuming the total current  $I$  flows uniformly on the outer surface of a hollow conductor with a circular cross-section of radius  $r_b$ . The shape of the hollow conductor is approximately that of the spacecraft surface. The inductance of such a device is given by<sup>38</sup>

$$L \approx \mu_0 r_c \left[ \ln \left( \frac{8r_c}{r_b} \right) - 2 \right] \quad (9)$$

where  $r_c$  is the radial distance to the approximate center of the circular cross-section. Using values for  $r_c$  in equation (9) and the corresponding current  $I$  from the three different shielded regions shown in Fig. 2, the approximate inductance and energy are calculated and shown in Table 1. A value of  $r_b = 2.5$  m was used in each case. The large energy required to power the shield is a significant drawback of this design, in addition to the dangers associated with quenching of the coils.

**Table 1. Energy Stored in Coils**

$r_c$ , m	$L$ , $\mu\text{H}$	$I$ MA	$E$ , GJ	$E$ , MWh
5.0	4.87	645	1013	281
10.0	18.5	169	263	73
15.0	35.4	107	203	56

There are other practical considerations that must be addressed such as the stresses the coils induce on each other and on the spacecraft. Because the current in each coil flows in the same direction, it is expected that an overall force is directed inward from the surface of the spacecraft. Additional structural reinforcement of the spacecraft could be required to withstand these forces. Furthermore, in these examples it was assumed that no magnetically permeable materials were present in calculating the magnetic fields. The presence of such materials would alter the resulting magnetic fields, perhaps significantly. A more detailed analysis of the effect of using magnetically permeable materials in the spacecraft would be required.

It is clear that there are numerous challenges to building a magnetic shield capable of protecting astronauts from GCR particles. Our intent is not to address all of these practical considerations, but rather to demonstrate that it is possible to construct a magnetic field, at least in principle, that is both strong enough to deflect incident GCR particles and at the same time low enough interior to the spacecraft so as not to cause undesirable physiological effects on the inhabitants. The toroidal design described here accomplishes these apparently contradictory requirements.

## V. Conclusion

We have proposed a novel concept for a magnetic spacecraft shield which has the desired features of effectively shielding energetic particles from a toroidal region of space while also maintaining a low (near zero) magnetic field in this region. The shape of the spacecraft is that of a torus with a cross section that is determined by the shape that a magnetic field-line from a circular coil of wire contained within the torus makes. By making the spacecraft conform to this special shape it is relatively easy to distribute electrical current in wires around the surface of the spacecraft such that the magnetic field inside is virtually eliminated. The resulting magnetic field can be designed to completely shield particles below a given energy, including GCR particles, from a region containing the spacecraft.

The boundaries of shielded regions are determined for several configurations using two different numerical

techniques. The first method involves numerically solving an equation that describes a constant of the motion of charged particles in a magnetic field,<sup>27</sup> including cases where the full vector potential due to multiple coils is required. The second method involves numerical solution of test particle trajectories in the same magnetic field. Excellent agreement between boundaries determined using both methods is shown to occur.

Toroidal spacecraft have been previously suggested and there are advantages to such a design.<sup>21–23, 35, 37, 39, 40</sup> Principle among these advantages is moving the habitation region away from a centralized region near the origin. Magnetic shields which are located near the origin of the magnetic field all suffer from the serious flaw that they cannot shield particles along the main axis of the field, thereby allowing particles from some directions to penetrate the spacecraft.<sup>20</sup> No such difficulties are encountered with toroidal spacecraft as particles approaching along the axis of the field pass harmlessly through the center of the torus.

While it has been demonstrated that a magnetic field configuration is possible, at least in principle, that is strong enough to effectively shield GCR particles and at the same time weak enough inside the spacecraft so as not to induce a harmful environment to astronauts, there are many practical concerns that must be addressed with this design. Foremost among these issues is the large electrical current ( $> 10^8$  A) and energy ( $> 10^{11}$  J) that is required to provide a magnetic field capable of shielding GCR particles. Whether it is possible to safely and practically generate a current of this magnitude, as well as other issues associated with currents of this magnitude, is a challenge that must be overcome for a magnetic spacecraft shield of this design to be considered and make extended duration manned missions a reality.

## Acknowledgments

We would like to thank Bengt U. Ö Sonnerup for his suggestions and encouragement in pursuing several critical aspects of the work presented here. This work was supported by NSF grant ATM-0519072, by NASA grants NNG056676H, and in part by the STC program of NSF under Agreement Number ATM-0120950.

## References

- <sup>1</sup>Chen, J., Chenette, D., Guzik, T. G., Garciamunoz, M., Pyle, K. R., Sang, Y., and Wefel, J. P., “A Model of Solar Energetic Particles for use in Calculating Let Spectra Developed from ONR-604 Data,” *Life Sci. Space Res.*, Vol. 14, No. 10, 1994, pp. 675–680.
- <sup>2</sup>Chen, J., Chenette, D., Clark, R., Garciamunoz, M., Guzik, T. G., Pyle, K. R., Sang, Y., and Wefel, J. P., “A Model of Galactic Cosmic-Rays for use in Calculating Linear-Energy-Spectra,” *Life Sci. Space Res.*, Vol. 14, No. 10, 1994, pp. 765–769.
- <sup>3</sup>Yao, W.-M. e. a., “Review of Particle Physics,” *J. Phys. G: Nucl. Part. Phys.*, Vol. 33, No. 1, 2006, pp. 245–251.
- <sup>4</sup>Wilson, J. W., Miller, J., Konradi, A., and Cucinotta, F. A., “Shielding strategies for human space exploration,” NASA Conference Publication 3360, 1997.
- <sup>5</sup>Cucinotta, F. A., Schimmerling, W., Wilson, J. W., Peterson, L. E., Badhwar, G. D., Saganti, P. B., and DiCello, J. F., “Space radiation cancer risks and uncertainties for Mars Missions,” *Radiation Res.*, Vol. 156, 2001, pp. 682–688.
- <sup>6</sup>Hoffman, J. A., Fisher, P., and Batishchev, O., “Use of Superconducting Magnet Technology for Astronaut Radiation Protection,” NIAC CP 04-01 Phase I Final Report, 2005.
- <sup>7</sup>Schimmerling, W. and Cucinotta, F. A., “Dose and does rate effectiveness of space radiation,” *Radiation Protection Dosimetry*, Vol. 122, No. 1–4, 2006, pp. 349–353.
- <sup>8</sup>Sussingham, J. C., Watkins, S. A., and Cocks, F. H., “Forty Years of Development of Active Systems for Radiation Protection of Spacecraft,” *J. Astronautical Sci.*, Vol. 47, No. 3–4, 1999, pp. 165–175.
- <sup>9</sup>Townsend, L. W., “Galactic Heavy-Ion Shielding Using Electrostatic Fields,” NASA Technical Memorandum 86255, 1984.
- <sup>10</sup>Buhler, C. R. and Wichmann, L., “Analysis of a Lunar Base Electrostatic Radiation Shield Concept,” NIAC CP 04-01 Phase I Final Report, 2005.
- <sup>11</sup>Winglee, R. M., “Advances in Magnetized Plasma Propulsion and Radiation Shielding,” Proceedings of the 2004 NASA/DoD Conference on Evolution Hardware (EH’04), IEEE, 2004.
- <sup>12</sup>Cocks, F. H., “A Deployable High Temperature Superconducting Coil (DHTSC): A Novel Concept for Producing Magnetic Shields Against Both Solar Flare and Galactic Radiation During Manned Interplanetary Missions,” *J. British. Interplanetary Soc.*, Vol. 44, 1991, pp. 99–102.
- <sup>13</sup>Townsend, L. W., “Overview of Active Methods for Shielding Spacecraft from Energetic Space Radiation,” 11<sup>th</sup> Annual NASA Space Radiation Health Investigators’ Workshop, Arona, Italy, 2000.
- <sup>14</sup>Kervendal, E. A., Kirk, D. R., and Meinke, R. B., “Spacecraft radiation shielding using ultra light-weight superconducting magnets,” AIAA 2007-497, 45th AIAA Aerospace Sciences Meeting and Exhibit, Reno, NV, 2007.
- <sup>15</sup>Parker, E. N., “Shielding Space Explorers from Cosmic Rays,” *Space Weather*, Vol. 3, 2005.
- <sup>16</sup>Cocks, J. C., Watkins, S. A., Cocks, F. H., and Sussingham, C., “Applications for Deployed High Temperature Superconducting Coils in Spacecraft Engineering: A Review and Analysis,” *J. British. Interplanetary Soc.*, Vol. 50, 1997, pp. 479–484.
- <sup>17</sup>Cocks, F. H. and Watkins, S., “Magnetic Shielding of Interplanetary Spacecraft Against Solar Flare Radiation,” NASA/USRA Advanced Design Program, Final Report, NASA-CR-195539, 1993.

- <sup>18</sup>Hilinski, E. J. and Cocks, F. H., “Deployed High-temperature Superconducting Coil Magnetic Shield,” *J. Spacecraft and Rockets*, Vol. 31, 1994, pp. 342.
- <sup>19</sup>Shepherd, S. G. and Kress, B. T., “Störmer Theory Applied to Magnetic Spacecraft Shielding,” *Space Weather*, Vol. 5, 2007.
- <sup>20</sup>Shepherd, S. G. and Kress, B. T., “Comment on “Applications for Deployed High Temperature Superconducting Coils in Spacecraft Engineering: A Review and Analysis” by J. C. Cocks et al.” *J. British. Interplanetary Soc.*, Vol. 60, 2007, pp. 129–132.
- <sup>21</sup>Levy, R. H., “Radiation Shielding of Space Vehicles by Means of Superconducting Coils,” *Amer. Rocket Soc.*, Vol. 31, No. 11, 1961, pp. 1568–1570.
- <sup>22</sup>Levine, S. H. and Lepper, R., “The Quasi-Hollow Conductor Magnet as a Space Shield Against Electrons,” *Trans. Amer. Nuclear Soc.*, Vol. 10, No. 1, 1967, pp. 377.
- <sup>23</sup>Braun, W. V., “Will Mighty Magnets Protect Voyagers to Planets?” *Popular Sci.*, 1969, pp. 98–100, 198.
- <sup>24</sup>Schenck, J. F., “Safety of Strong, Static Magnetic Fields,” *J. Magnetic Resonance Imaging*, Vol. 12, 2000, pp. 2–19.
- <sup>25</sup>de Vocht, F., van Drooge, H., Engels, H., and Kromhout, H., “Exposure, Health Complaints and Cognitive Performance Among Employees of an MRI Scanners Manufacturing Department,” *J. Magnetic Resonance Imaging*, Vol. 23, 2006, pp. 197–204.
- <sup>26</sup>Orear, J., Rosenfeld, A. H., and Schluter, R. A., *Nuclear physics: a course given by Enrico Fermi at the University of Chicago*, Univ. of Chicago Press, Chicago, Ill., pp. 224–230, 1950.
- <sup>27</sup>Levy, R. H., “Radiation Shielding of Space Vehicles by Means of Superconducting Coils,” Afsd-tn-61-7, Avco-Everett Research Lab. Research Report 106, 1961.
- <sup>28</sup>Urban, E. W., “Critical Störmer Conditions in Quadrupole and Double Ring-Current Fields,” *J. Math. Phys.*, Vol. 6, No. 12, 1965, pp. 1966–1975.
- <sup>29</sup>Panofsky, W. K. H. and Phillips, M., *Classical Electricity and Magnetism*, Addison-Wesley, Reading, Massachusetts, 2nd ed., p. 429, 1962.
- <sup>30</sup>Störmer, C., *The Polar Aurora*, Oxford Univ. Press, pp. 229–246, 1955.
- <sup>31</sup>Levy, R. H., “Plasma Radiation Shielding,” *AIAA J.*, Vol. 2, No. 10, 1964, pp. 1835–1838.
- <sup>32</sup>Smart, D. F., Shea, M. A., and Fluckiger, E. O., “Magnetospheric models and trajectory computations,” *Space Sci. Rev.*, Vol. 93, No. 1–2, 2000, pp. 305–333.
- <sup>33</sup>Kress, B. T., Hudson, M. K., Perry, K. L., and Slocum, P. L., “Dynamic Modeling of Geomagnetic Cutoff for the 23–24 November 2001 Solar Energetic Particle Event,” *Geophys. Res. Lett.*, Vol. 31, 2004.
- <sup>34</sup>“Static Fields,” Environmental Health Criteria Monograph No. 232, World Health Organization, Geneva, Switzerland, 2006.
- <sup>35</sup>Parker, E. N., “Shielding Space Travelers,” *Sci. Amer.*, Vol. 294, No. 3, 2006, pp. 40–47.
- <sup>36</sup>Reitz, J. R., Milford, F. J., and Christy, R. W., *Foundations of Electromagnetic Theory*, Addison-Wesley, Reading, Massachusetts, 3rd ed., pp. 201–203, 1980.
- <sup>37</sup>Levine, S. H. and Lepper, R., “Analog Studies of Magnetic Shields,” *AIAA J.*, Vol. 6, No. 4, 1968, pp. 695–701.
- <sup>38</sup>Harwell, G. P., *Principles of Electricity and Magnetism*, McGraw-Hill, New York, 2nd ed., pp. 324–330, 1949.
- <sup>39</sup>Keffer, C. O., “Experimental Investigation of Packaging and Deployment Characteristics of an Inflatable Toroidal-Space Station Configuration,” NASA-TM-X-1079, April, 1965.
- <sup>40</sup>Levy, R. H. and French, F. W., “Plasma Radiation Shield: Concept and Applications to Space Vehicles,” *J. Spacecraft*, Vol. 5, No. 5, 1968, pp. 570–577.

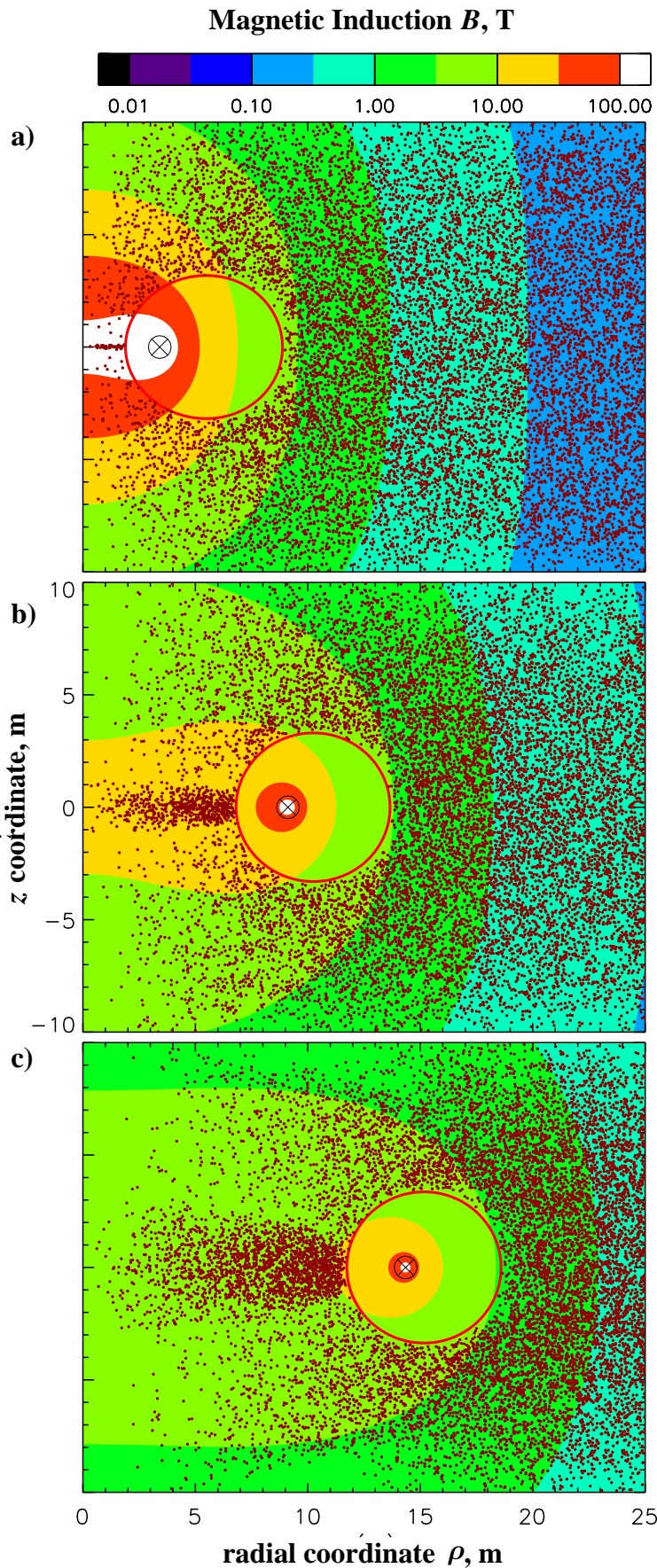


Figure 2. Shielded regions for single coils of three different radii  $a =$  (a) 3.415 m, (b) 9.115 m, and (c) 14.35 m are indicated by the thick solid white line containing a thinner dashed black line. The location of the wire is indicated by the circular symbol with a cross. The shielded region shown in each case is for protons with energy 1 GeV. The current required in each coil to shield these particles is  $nI = 6.451 \times 10^8$  A,  $1.688 \times 10^8$  A, and  $1.071 \times 10^8$ , respectively. The magnitude of the magnetic field is shown by the logarithmic greyscale. Positions of the closest approach to the coil of test particles, shown as dots, confirm the existence of the forbidden region.

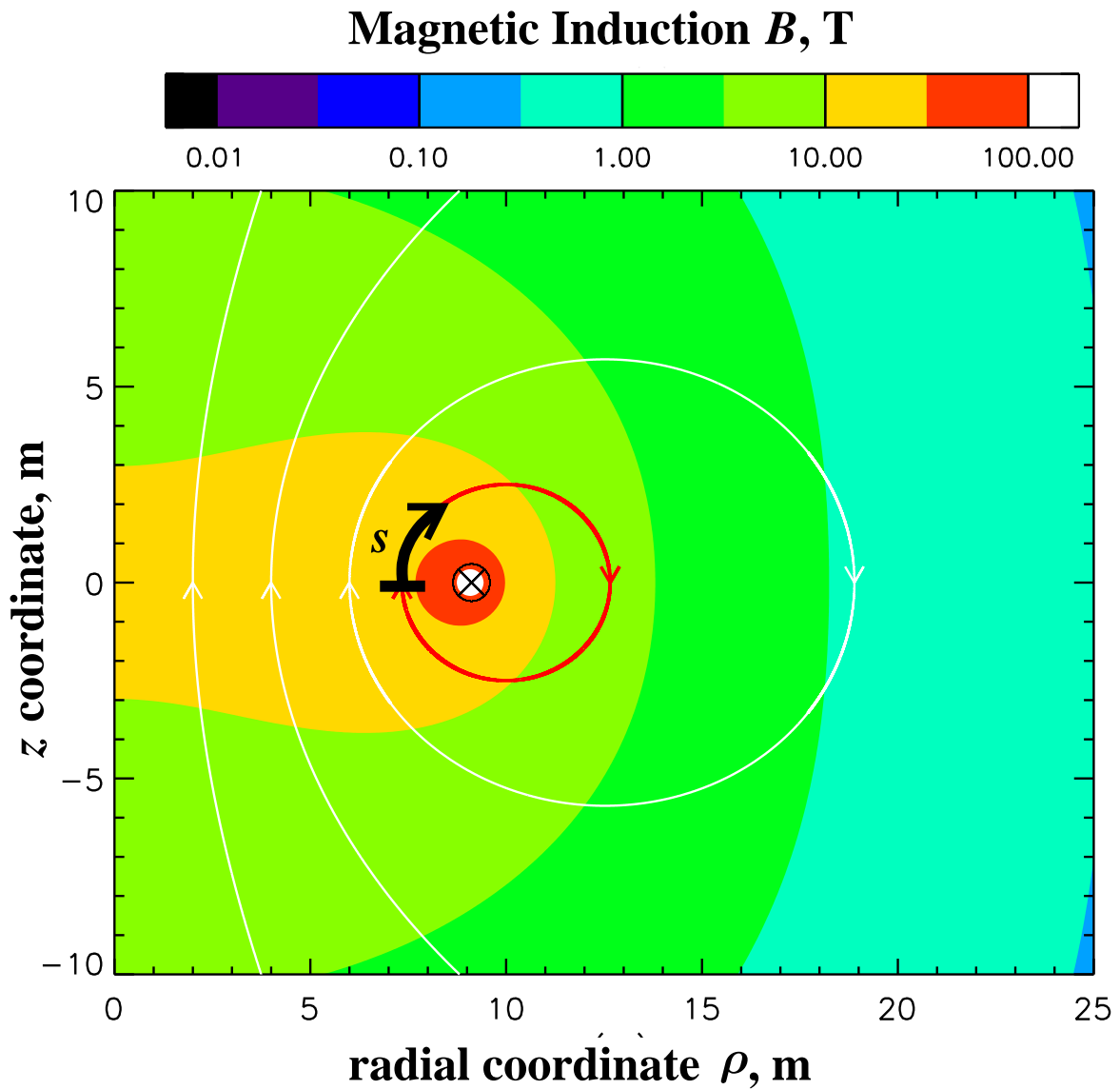


Figure 3. Magnetic field-strength for a single coil of wire shown in Fig. 2b. Representative magnetic field-lines are shown. The cross-section of the spacecraft is described by the field-line closest to the coil indicated by the thicker line. Distance along the field-line is indicated by  $s$ .

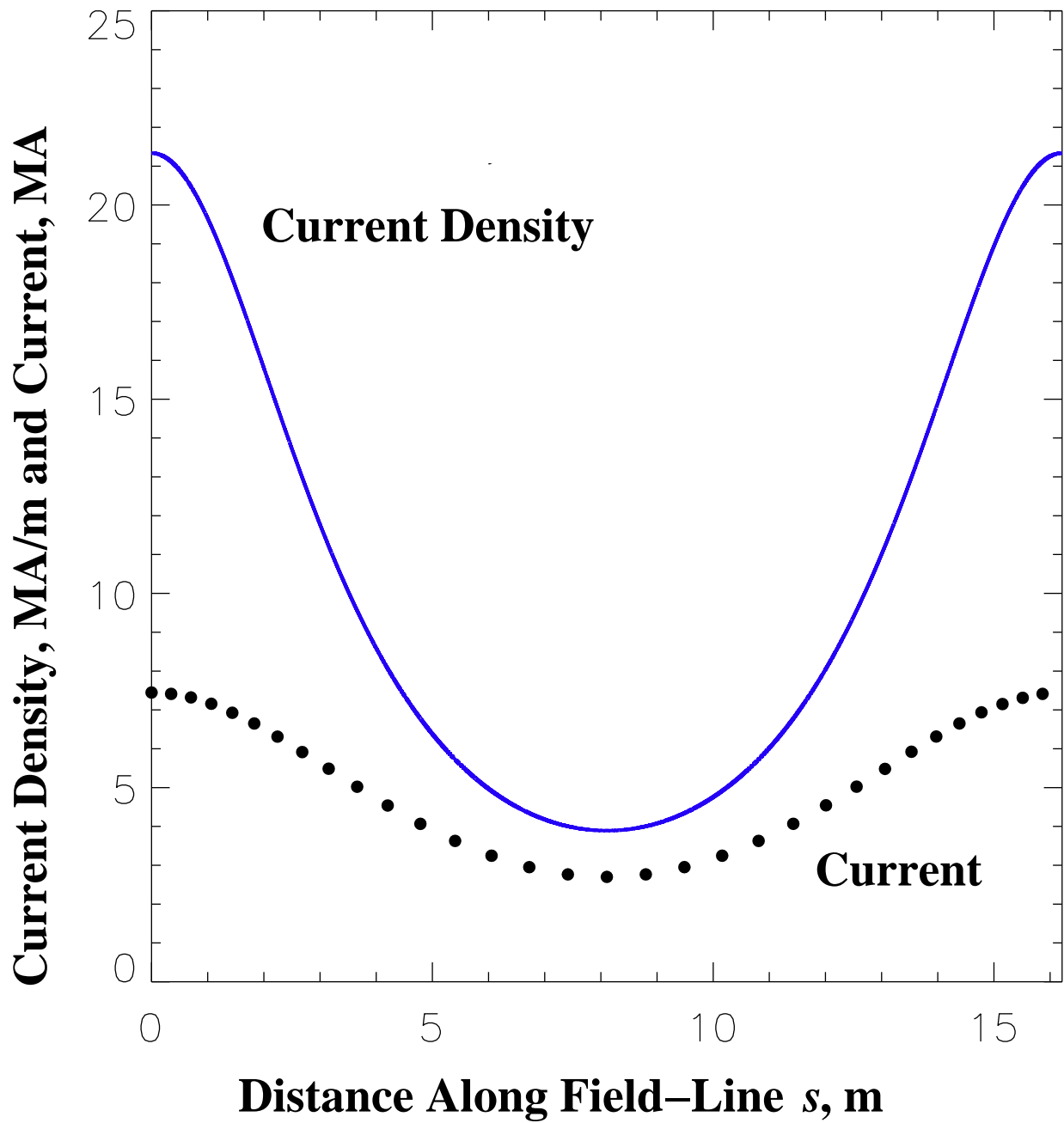


Figure 4. Surface current density (solid line) as function of distance along the field-line ( $s$ ). Dots indicate the positions and current amplitudes of 32 discrete wires distributed around the field-line.

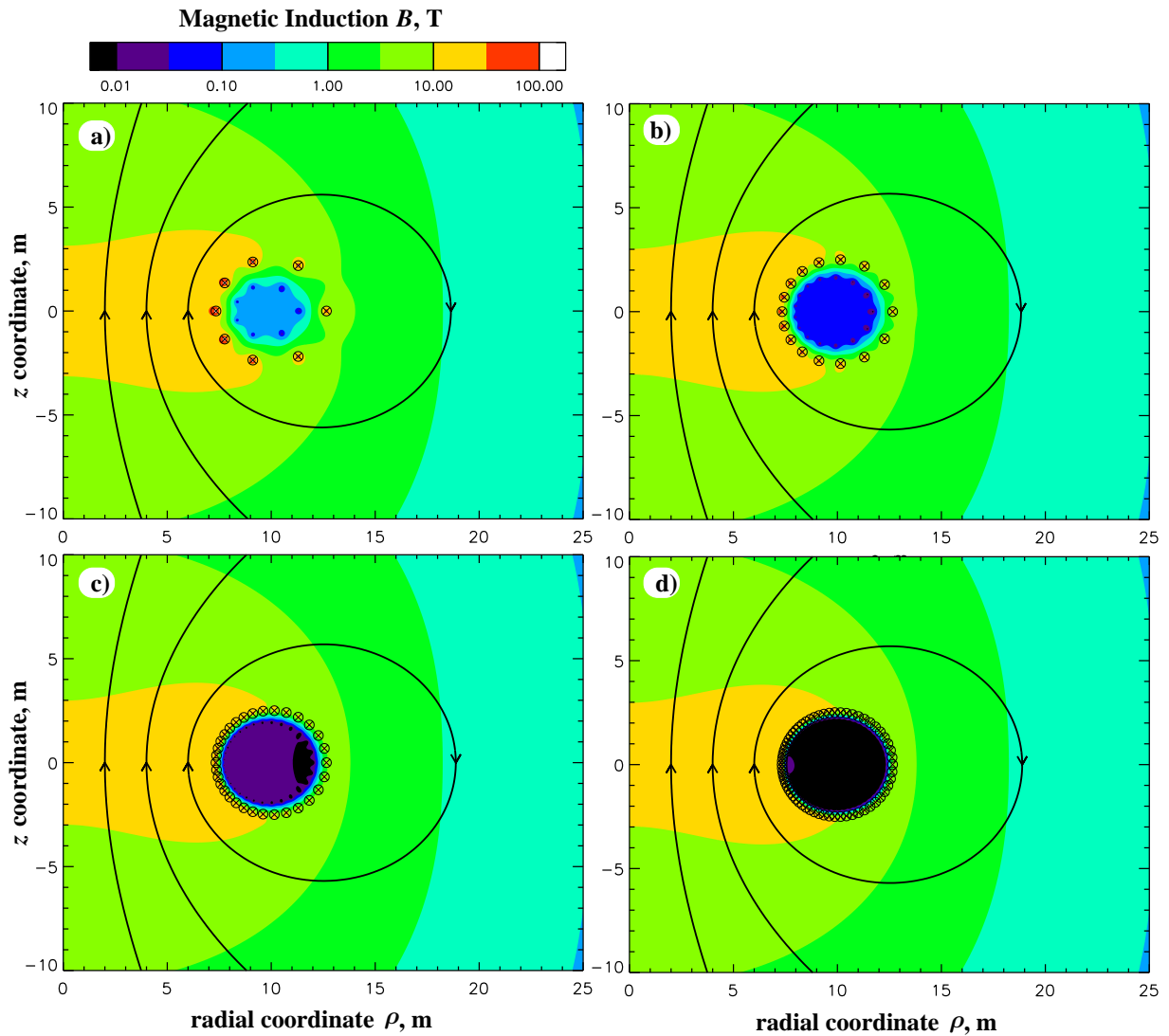


Figure 5. Magnetic field-strength shown as a logarithmic greyscale for (a) 8-coil, (b) 16-coil, (c) 32-coil, and (d) 64-coil approximations to equation (8). Locations of the coils are indicated by the circular symbol with a cross. The current in each coil is determined by the curves in Fig. 4. Representative magnetic field-lines are shown as solid lines with arrows.

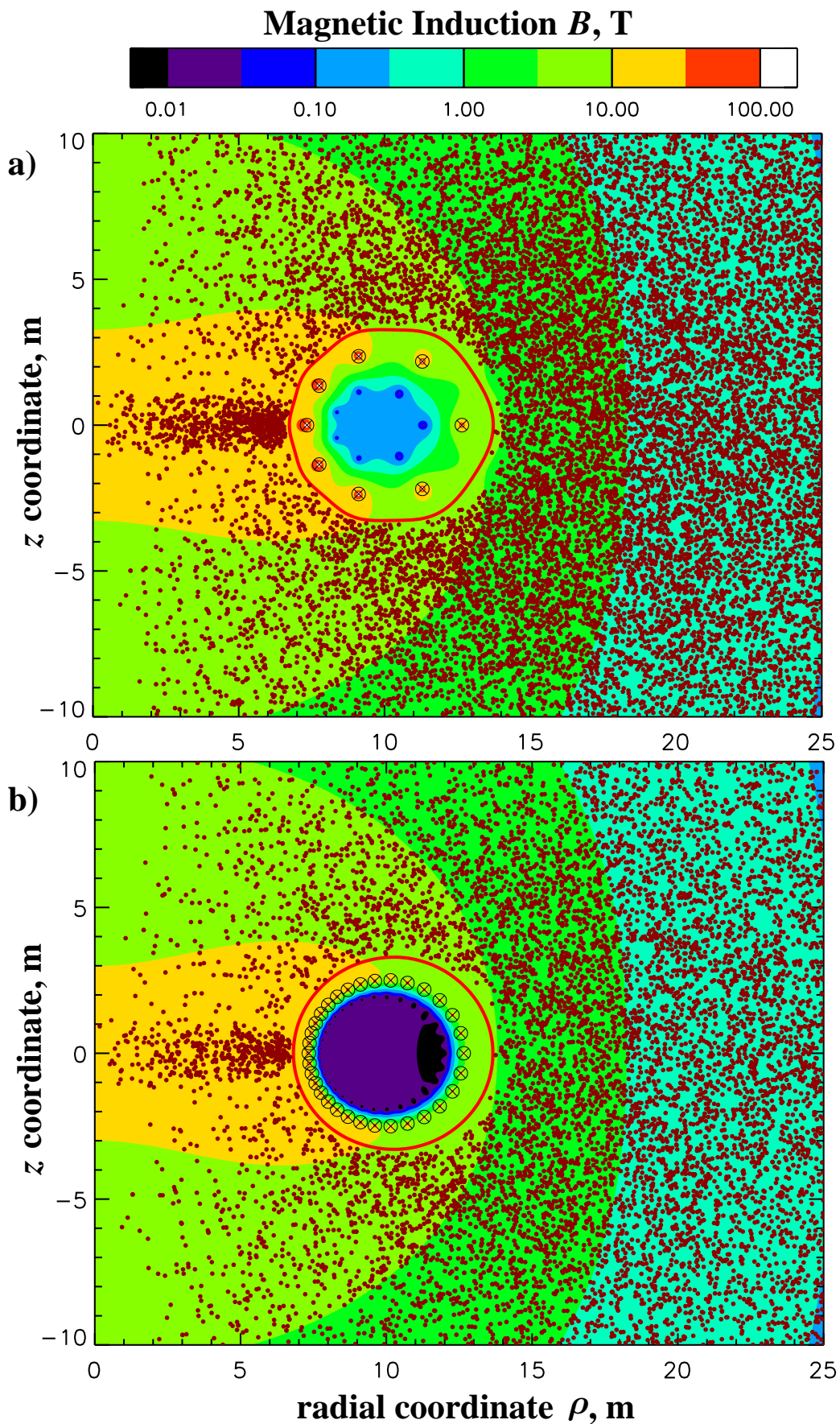


Figure 6. Shielded regions computed using the full vector potential  $A_\phi$  of the (a) 8-coil and (b) 32-coil configurations showing good agreement with test-particle simulations.

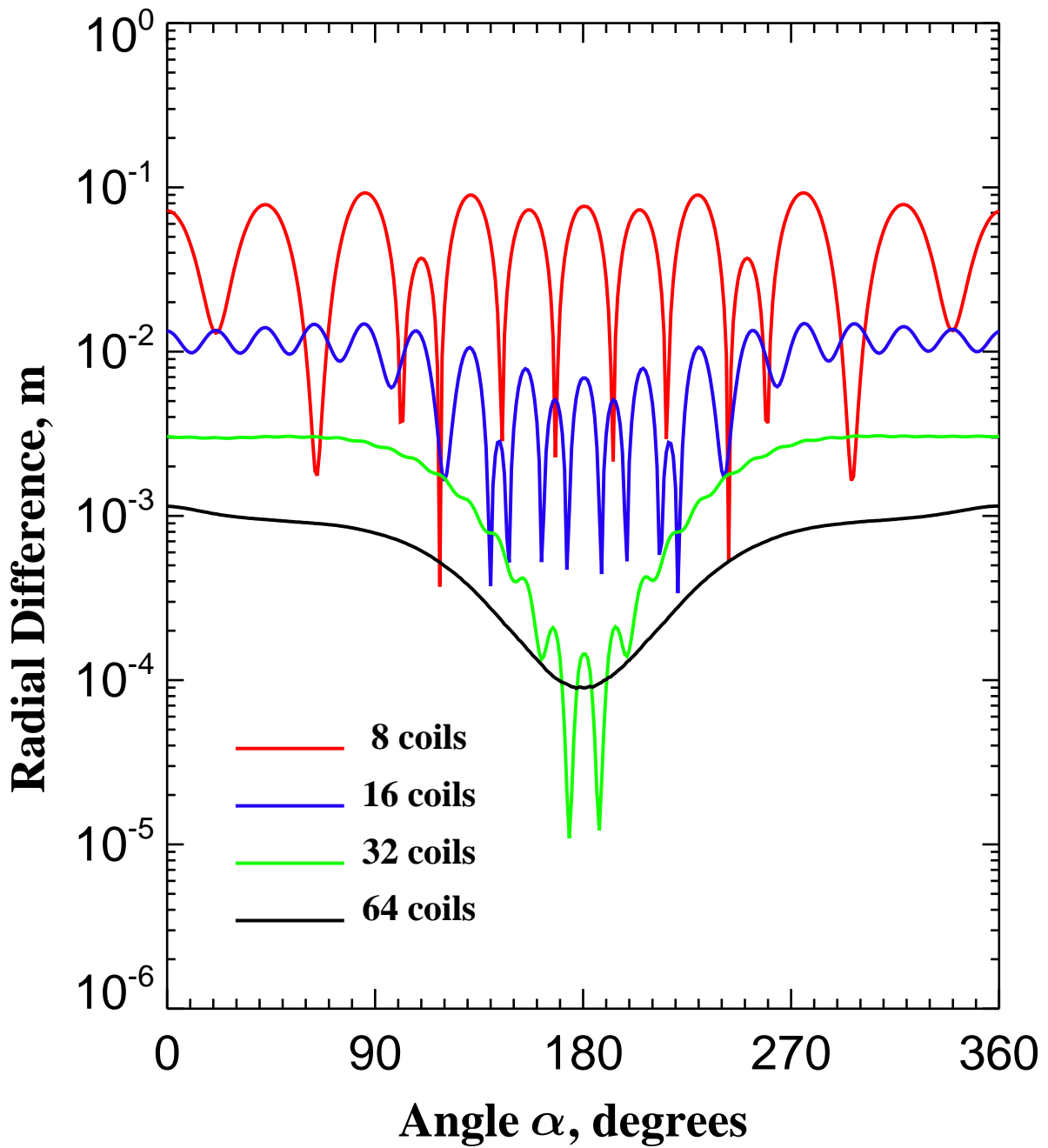


Figure 7. Radial differences between the shielded regions computed using the single wire vector potential and the exact vector potential for the various multiple-coil configurations.